

Constraining stress magnitudes using petroleum exploration data in the Cooper–Eromanga Basins, Australia

Scott D. Reynolds^{a,*}, Scott D. Mildren^{a,1}, Richard R. Hillis^a, Jeremy J. Meyer^b

^a Australian School of Petroleum, The University of Adelaide, 5005 Australia

^b JRS Petroleum Research Pty Ltd., PO Box 319, Kent Town, 5071 Australia

Received 7 July 2005; received in revised form 2 December 2005; accepted 21 December 2005

Available online 23 February 2006

Abstract

The magnitude of the in situ stresses in the Cooper–Eromanga Basins have been determined using an extensive petroleum exploration database from over 40 years of drilling. The magnitude of the vertical stress (S_v) was calculated based on density and velocity checkshot data in 24 wells. Upper and lower bound values of the vertical stress magnitude are approximated by $S_v = (14.39 \times Z)^{1.12}$ and $S_v = (11.67 \times Z)^{1.15}$ functions respectively (where Z is depth in km and S_v is in MPa). Leak-off test data from the two basins constrain the lower bound estimate for the minimum horizontal stress (S_{hmin}) magnitude to 15.5 MPa/km. Closure pressures from a large number of minifrac tests indicate considerable scatter in the minimum horizontal stress magnitude, with values approaching the magnitude of the vertical stress in some areas. The magnitude of the maximum horizontal stress (S_{Hmax}) was constrained by the frictional limits to stress beyond which faulting occurs and by the presence of drilling-induced tensile fractures in some wells. The maximum horizontal stress magnitude can only be loosely constrained regionally using frictional limits, due to the variability of both the minimum horizontal stress and vertical stress estimates. However, the maximum horizontal stress and thus the full stress tensor can be better constrained at individual well locations, as demonstrated in Bulyeroo-1 and Dullingari North-8, where the necessary data (i.e. image logs, minifrac tests and density logs) are available. The stress magnitudes determined indicate a predominantly strike-slip fault stress regime ($S_{Hmax} > S_v > S_{hmin}$) at a depth of between 1 and 3 km in the Cooper–Eromanga Basins. However, some areas of the basin are transitional between strike-slip and reverse fault stress regimes ($S_{Hmax} > S_v \approx S_{hmin}$). Large differential stresses in the Cooper–Eromanga Basins indicate a high upper crustal strength for the region, consistent with other intraplate regions. We propose that the in situ stress field in the Cooper–Eromanga Basins is a direct result of the complex interaction of tectonic stresses from the convergent plate boundaries surrounding the Indo-Australian plate that are transmitted into the center of the plate through a high-strength upper crust.

© 2006 Elsevier B.V. All rights reserved.

Keywords: Cooper–Eromanga Basins; Stress magnitudes; Tectonic regime; Crustal strength

1. Introduction

The Cooper–Eromanga Basins are located in central Australia and provide an ideal location to study the in situ stress field in an intraplate setting due to the extensive amount of available petroleum exploration data (Fig. 1). The Cooper Basin is a late Carboniferous

* Corresponding author. Tel.: +61 8 8303 4293; fax: +61 8 8303 4345.

E-mail address: reynolds@asp.adelaide.edu.au (S.D. Reynolds).

¹ Now at: JRS Petroleum Research Pty Ltd., PO Box 319, Kent Town, 5071 Australia.

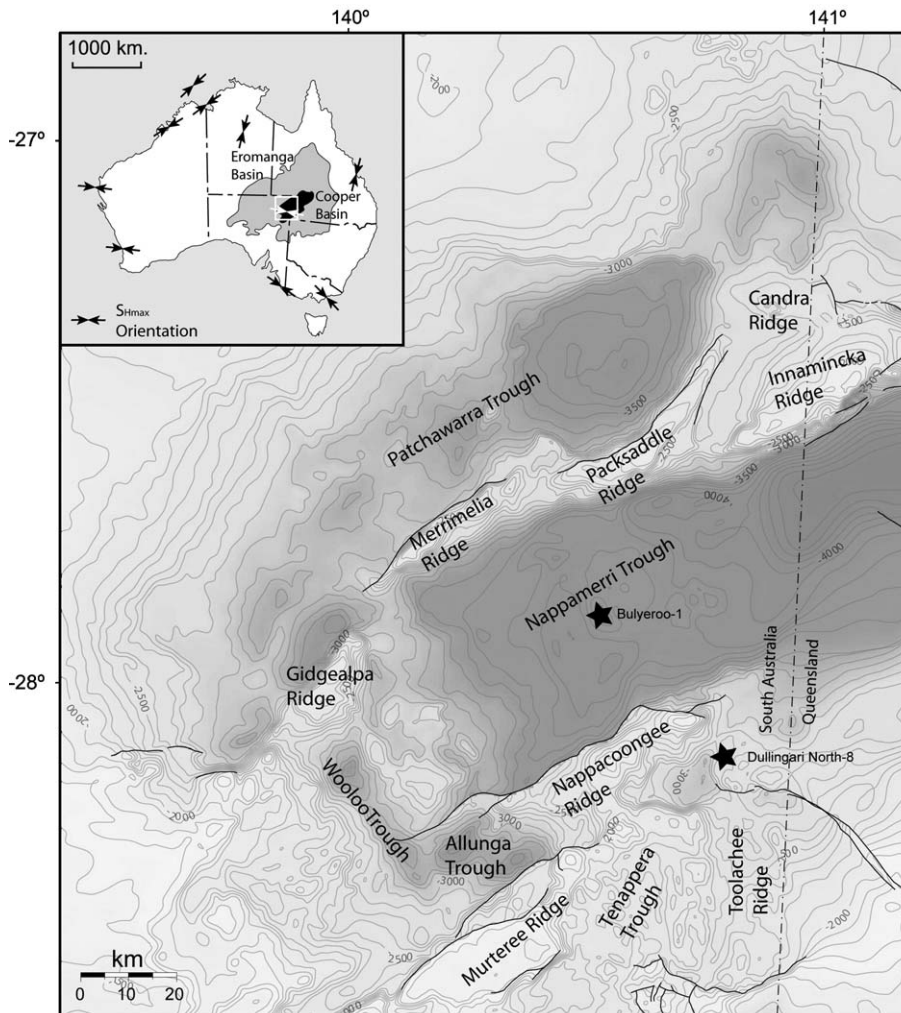


Fig. 1. Depth to basement (m) of the Cooper Basin showing major basement-cutting faults and structural elements. Well locations for Bulyeroo-1 and Dulligari North-8 are also shown. The insert map displays the regional stress orientations across Australia and the extent of the Cooper–Eromanga Basins.

to Middle Triassic basin separated by a major unconformity from the overlying and more laterally extensive, Jurassic to Cretaceous Eromanga Basin. Present-day stress data from these basins is of particular importance because of the relative paucity of stress data available for central Australia (Hillis and Reynolds, 2000). A previous study by Reynolds et al. (2005) has comprehensively described the maximum horizontal stress orientation throughout the Cooper–Eromanga Basins. The majority of the area exhibits an east–west maximum horizontal stress orientation, which was determined from the occurrence of borehole breakouts and drilling-induced tensile fractures interpreted from dipmeter and image logs (Reynolds et al., 2005). The consistency in the maximum horizontal stress orientation across the basin indicates a tectonic and/or regional source of stress

controlling the stress field, resulting in highly anisotropic horizontal stresses. However, the maximum horizontal stress orientation in the Cooper Basin is approximately perpendicular to the direction of absolute plate velocity for the Indo-Australian plate, indicating that the stress field is the result of the complex interaction of a number of large-scale forces (Reynolds et al., 2003, 2005). In this study we have analysed the stress magnitude data for the Cooper Basin in order to verify the anisotropic nature of the horizontal stresses and to investigate any observable trends in the magnitude data.

The Cooper–Eromanga Basins are Australia's largest onshore oil and gas province (Fig. 1). Since the first natural gas discovery in 1963, over 1200 wells have been drilled in the South Australian sector alone. In this

study we examine data from only the South Australian section of the two basins, which has the greatest concentration of wells (Fig. 1). The majority of the reservoirs in the Cooper Basin are tight (low permeability) and hence enhanced oil recovery, using techniques such as fracture stimulation, are important. However, not all hydraulic fracture stimulation results have been successful (Johnson and Greenstreet, 2003; Roberts et al., 2000). A number of problems have occurred during hydraulic fracture stimulation including near wellbore hydraulic fracture complexity (e.g. fracture twisting and multiple fractures) and high fracturing pressures (Chipperfield and Britt, 2000; Johnson et al., 2002; Roberts et al., 2000). These problems have been attributed to a high stress environment and low permeability reservoirs in the basin (Johnson et al., 2002; Johnson and Greenstreet, 2003). In recent years the Cooper–Eromanga Basins have been the focus for hot dry rock (HDR) geothermal energy exploration. The area has high heat flows and contains Australia’s most significant geothermal resource recognised to date (Somerville et al., 1994; Wyborn et al., 2004).

In this study we have used the petroleum exploration data to constrain the magnitude of the vertical stress, the minimum horizontal stress and the maximum horizontal stress to a depth of 3 km. The pore pressure distribution across the two basins has also been investigated, as any overpressure or underpressure has significant implications for the stress magnitudes. In this study we have broadly constrained the stress magnitudes across the two basins as a whole, as well as determining the full stress tensor at the Bulyeroo-1 and Dullingari North-8 wells. These two wells were selected because they have reasonably complete data sets available, as is required to determine the full stress tensor and they are located in different structural settings within the Cooper–Eromanga Basins.

The stress magnitudes calculated in this study clearly indicate that the differential stress in the Cooper–Eromanga Basins is substantial. High differential stresses may indicate stress amplification in the upper crust, as a result of creep and stress decay in the lower crust and upper mantle (Kusznir and Bott, 1977; Mithen, 1982). This result implies that the upper crustal strength in the region is high (Zoback et al., 1993, 2002). A high-strength upper crust provides an efficient means to transfer tectonic stresses from the plate boundaries into intraplate regions (Zoback et al., 2002). We discuss the implication of the high-strength upper crust in terms of possible plate boundary forces acting on the Indo-Australian plate. Finally we discuss the apparent lack of deformation in the Cooper–Eromanga Basins compared

to other areas of Australia, despite the high differential stress.

2. Geological setting

The Cooper Basin is a Late Carboniferous to Middle Triassic, non-marine sedimentary basin, up to 4.5 km deep, located in central Australia (Hill and Gravestock, 1995). Only the South Australian sector, which makes up one-third of the basin (35,000 km²), is evaluated in this stress study (Fig. 1). The South Australian sector of the basin contains the greatest thickness of hydrocarbon-bearing Permian strata and hence the largest amount of well data (Gravestock and Jensen-Schmidt, 1998). A major unconformity occurs at the top of the Cooper Basin, separating it from the overlying Eromanga Basin of Jurassic to Cretaceous age (Apak et al., 1997) (Fig. 2).

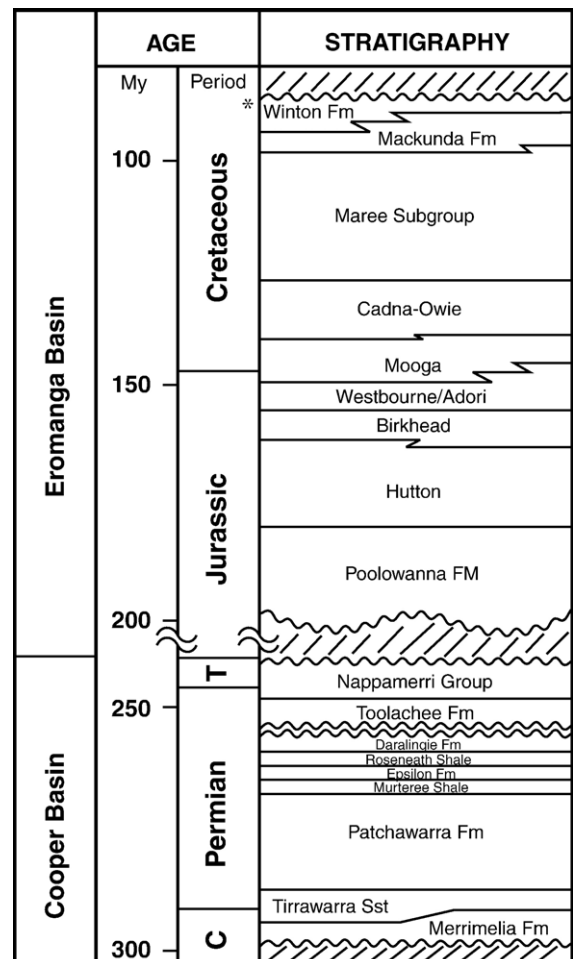


Fig. 2. Stratigraphy of the Cooper–Eromanga Basins. The unconformity at the top of the Eromanga Basin (*) marks the base of the Tertiary Lake Eyre Basin. T: Triassic, C: Carboniferous.

The depth to this unconformity varies from 970 m to 2800 m below sea level (Laws and Gravestock, 1998). Another major unconformity separates the Jurassic to Cretaceous Eromanga Basin from the Tertiary Lake Eyre Basin, which is typically 100–200 m thick in the area of study.

In Australian terminology, overlying successor basins are generally given different names. The Eromanga Basin is a widespread successor basin overlying the Cooper Basin (Fig. 1). The Tertiary Lake Eyre Basin covers a broadly similar area of South Australia as the Eromanga Basin. The majority of the stress data included herein come from the Cooper and Eromanga Basins, although vertical stress data, for example, also sample the Tertiary Lake Eyre Basin. For the sake of simplicity we refer to this study as covering the Cooper–Eromanga Basins. Indeed the study only covers the Eromanga Basin within the geographic area of subcrop of the Cooper Basin.

The South Australian sector of the Cooper Basin, which is the major focus of petroleum exploration, comprises a series of northeast to southwest trending ridges and troughs (Fig. 1). The major depocenters include the Patchawarra Trough, the Nappamerri Trough and the Tennapera Trough, which are separated by two major intrabasin highs, the Gidgealpa-Merrimelia-Innamincka (GMI) Ridge and the Muteree-Nappa-coongee Ridge (Fig. 1). A northeast structural grain dominates the South Australian sector of the Cooper Basin.

3. Pore pressure

Knowledge of pore pressure is required for the determination of stress magnitudes in the Cooper–Eromanga Basins. A number of direct pressure measurements have been undertaken in the Cooper–Eromanga Basins. These measurements include drill stem tests (DSTs) and repeat formation tests (RFTs). Direct pressure measurements provide the most accurate pore pressure estimates. However, their spatial and depth distribution is often limited. Mud weight can, with caution, be used as a proxy for pore pressure, as mud weight is often just in excess of pore pressure to avoid drilling problems and to maximise drilling efficiency. Care must be exercised to ensure any increases in mud weight are due to pore pressure changes and not, for example, to address wellbore stability issues. van Ruth and Hillis (2000) compared DST pressures with mud weights used during drilling in the Cooper–Eromanga Basins and showed that mud weights do accurately reflect pore pressure in reservoir units. Thus, in the

absence of direct pressure data mud weights have been used as a proxy for pore pressure.

The available pore pressure data indicate that the Cooper–Eromanga Basins are generally hydrostatically pressured (Fig. 3). However, a number of wells do indicate significant overpressures, which start at a depth of around 2700 m (Fig. 3). These wells include McLeod-1, Bulyeroo-1, Kirby-1, Burley-1, Burley-2 and Moomba-55, which are all located in the Nappamerri Trough (van Ruth and Hillis, 2000). Overpressure occurs in the Toolachee Formation and deeper units of the Cooper Basin (van Ruth and Hillis, 2000).

In this study the complete stress tensor has been determined for Dullingari North-8 assuming hydrostatic pore pressure. We have also calculated the complete stress tensor for Bulyeroo-1 assuming the pore pressure is equal to the mud weight (overpressured). A number of direct pressure measurements, largely from the Moomba Field, indicate underpressure, which is a result of draw down due to extensive hydrocarbon production in the basin over the past 40 years. Stress measurements undertaken in depleted fields were specifically excluded from this study.

4. Vertical stress magnitude

The vertical, or overburden stress (S_v) at a specified depth can be equated with the pressure exerted by the weight of the overlying rocks and expressed as:

$$S_v = \int_0^z \rho(z)g dz, \quad (1)$$

where $\rho(z)$ is the density of the overlying rock column at depth z , and g is the acceleration due to gravity. Vertical stress profiles were generated after first filtering each density log to remove spurious data due to poor hole conditions. Filtering used a cut off of $\pm 0.05 \text{ g/cm}^3$ from the DRHO (density correction) curve and $\pm 5\%$ of bit size determined from the caliper data. A significant number of coal beds occur throughout the basins and pose problems when attempting to calculate the vertical stress because they are invariably associated with poor hole conditions. Systematically ignoring the coals, due to the poor hole conditions (giving unreliable density log data) with which they are associated, would lead to anomalously high sediment density/vertical stress because coals have very low density. In order to address this issue, coals were identified by their combined sonic ($DT > 90 \text{ } \mu\text{s/m}$) and gamma ray ($GR < 90 \text{ API units}$) response and were assigned a density of 1.32 g/cm^3 based on knowledge of coal density.

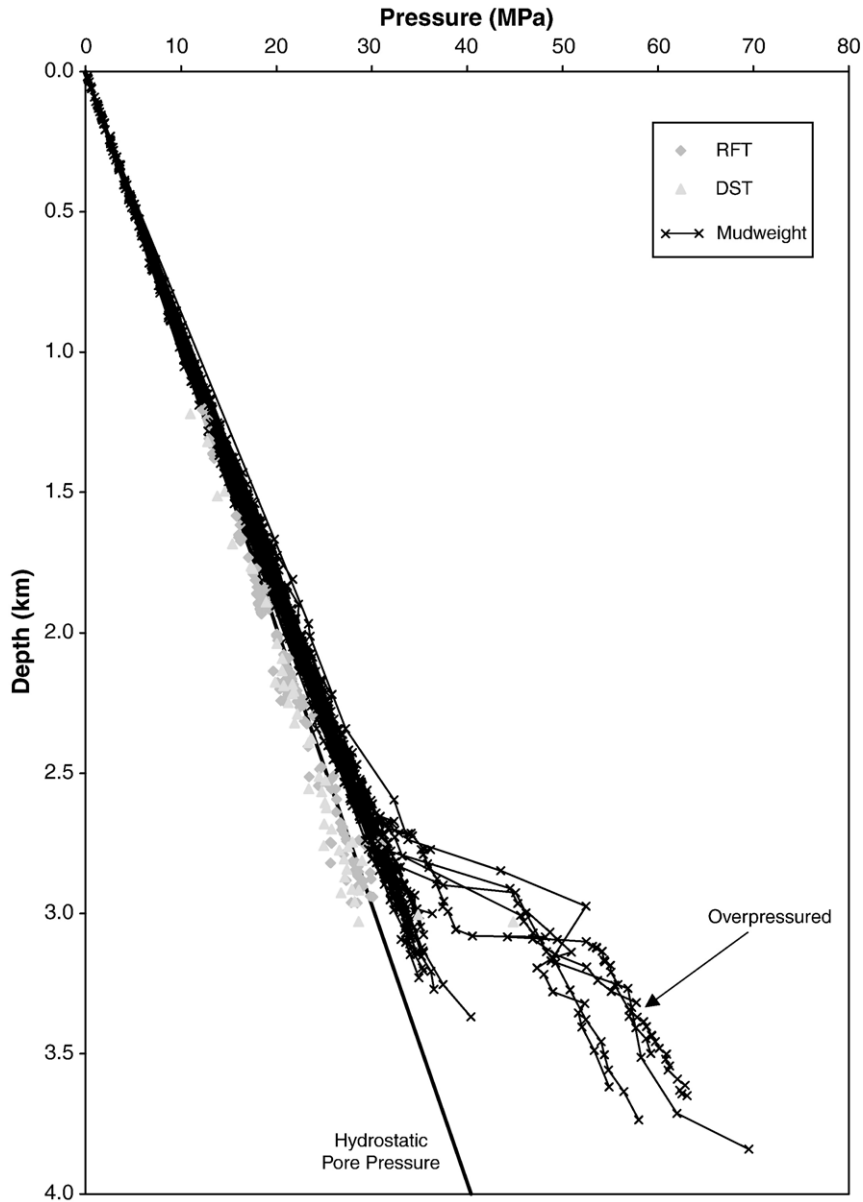


Fig. 3. Pore pressure versus depth compilation for the Cooper–Eromanga Basins. RFT: Repeat Formation Test, DST: Drill Stem Test.

Vertical stress calculations require that the density log be integrated from the surface. However, the density logs are not commonly run from the surface. The average density from the surface to the top of the density log run was estimated by converting checkshot velocity data to density using the Nafe-Drake velocity/density transform (Ludwig et al., 1970).

Vertical stress profiles were calculated for 24 wells evenly dispersed across the basins (Fig. 4). A significant degree of scatter is apparent in the vertical stress profiles from the 24 wells (Fig. 4). There is no discernible geographic/geological pattern in the variation of the

vertical stress. Power law functions most accurately approximate the upper and lower bounds to the vertical stress (S_v) in the Cooper–Eromanga Basins and have the form:

$$S_v = (11.67 \times Z)^{1.15} \quad \text{Lower bound} \quad (2)$$

$$S_v = (14.39 \times Z)^{1.12} \quad \text{Upper bound} \quad (3)$$

where S_v is in MPa and Z is the depth in km below land surface. It is preferable to use the vertical stress values calculated at the actual well or from a nearby well for

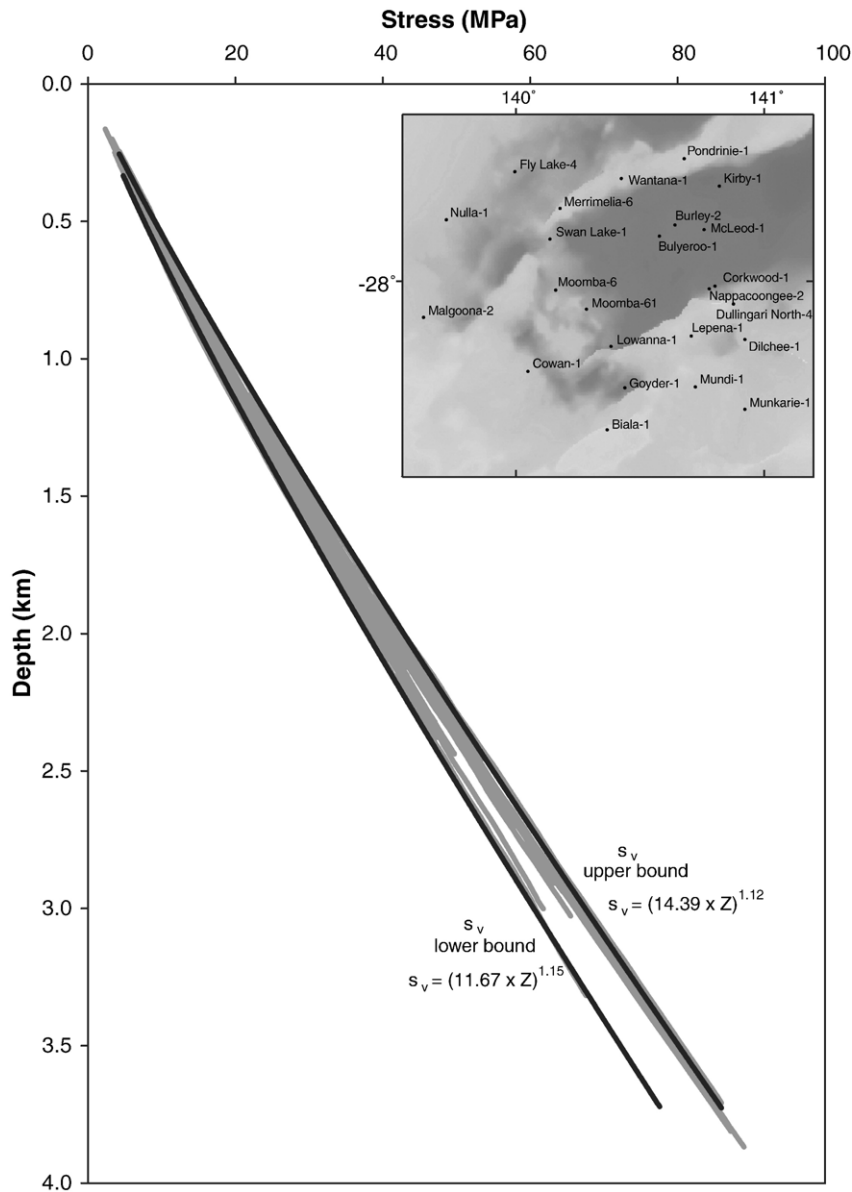


Fig. 4. Vertical stress (S_v) versus depth compilation for the Cooper–Eromanga Basins. Grey profiles indicate S_v in individual wells. Darker lines indicate basin-wide upper and lower bound estimates. Insert map showing individual wells used for S_v calculations.

detailed local studies, as subsequently demonstrated in this paper.

5. Minimum horizontal stress magnitude

The minimum horizontal stress (S_{hmin}) magnitude in petroleum basins is commonly determined using hydraulic fracture-type tests and leak-off tests (LOTs). Small volume, hydraulic fracture-type tests, referred to as minifrac in the petroleum industry, are pumping tests usually conducted in the design and execution of large-

scale fracture stimulation jobs. A minifrac test creates a fracture perpendicular to the minimum principal stress (the minimum horizontal stress in either a strike-slip or normal stress regime) by increasing the pressure in an isolated section of the wellbore. After the fracture is created the pumps are stopped and the test interval is shut-in. The pressure in the wellbore initially declines rapidly, eventually slowing down and coming to an equilibrium pressure above hydrostatic (Fig. 5). During this pressure decline the newly created fracture closes. The closure pressure corresponds to the instant when the

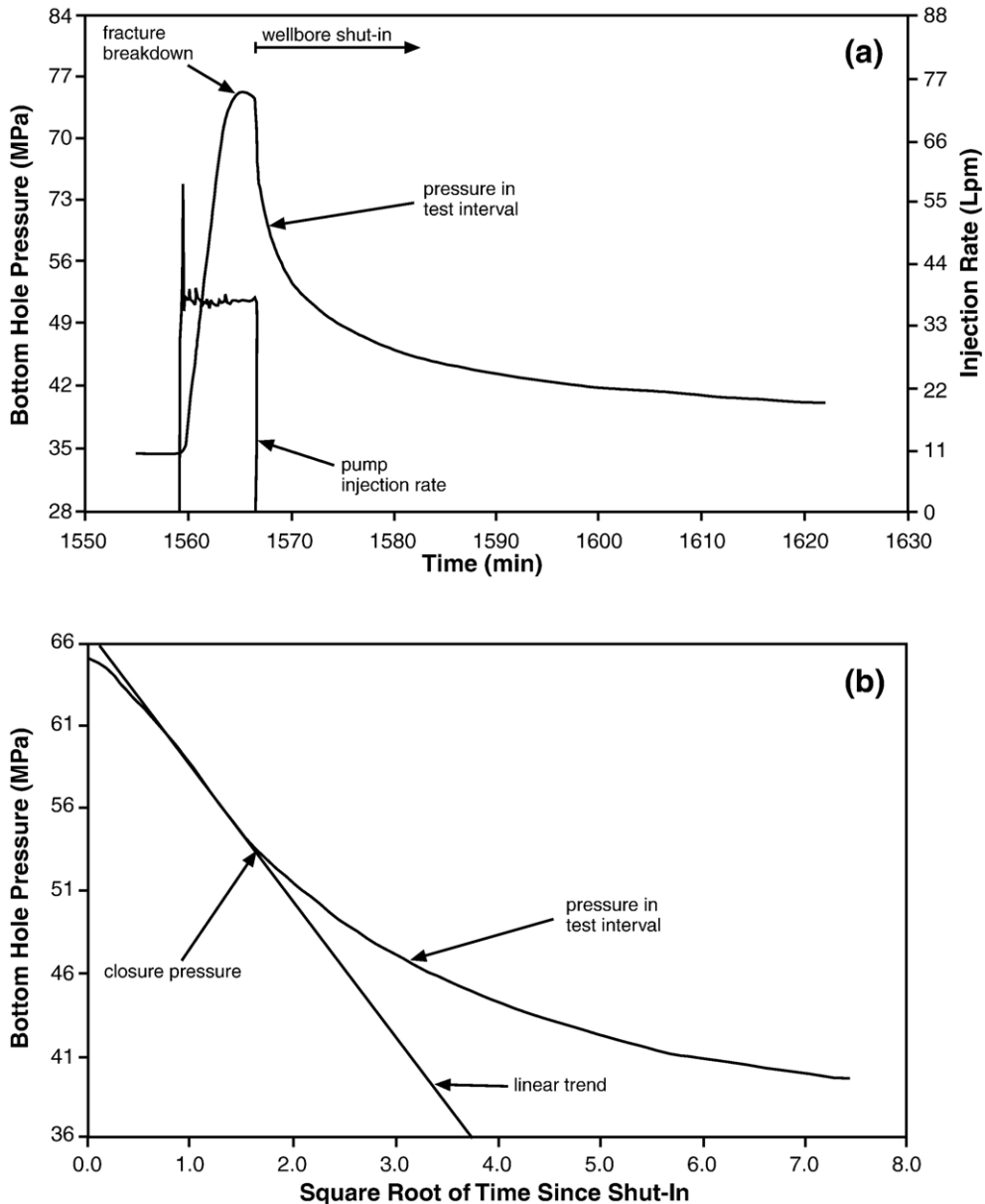


Fig. 5. (a) Example of a minifrac test conducted in Bulyeroo-1. Graph represents one cycle of a pump-in/shut-in test. Fracture closure occurs sometime after wellbore shut-in. (b) Closure pressure determined from the square root of time plot as described by Enever (1993). Closure pressure marked by the departure from the linear trend of the pressure in the test interval since shut-in.

walls of the fracture initially touch and hence equals the magnitude of the minimum principal stress (Gronseth and Kry, 1983). The fracture closure pressure is interpreted from the pressure record, as the point after shut-in at which there is a sudden decrease in the rate of pressure decline. It is often not clear on the pressure record where the closure pressure occurs, especially in permeable formations. However, displaying the pressure in the test interval against the square root of time after

shut-in can help identify the point of fracture closure (Enever, 1993) (Fig. 5b).

A large number of leak-off tests (LOTs) have been conducted in the two basins. Leak-off tests are commonly carried out during drilling operations to determine the maximum mud weight that can be used to drill the next section of the wellbore. Fluid is pumped into the wellbore, increasing the pressure, until the rate of pressurisation decreases (i.e. leak-off occurs). They

are similar only to the first stage of the minifrac test. The fluid leak-off represents the point of fracture initiation and corresponds to a departure from linearity on the pressure versus time plot. Leak-off pressures do not yield as reliable an estimate of the minimum horizontal stress magnitude as those determined from minifrac tests. This is largely because the disturbed stress field at the wellbore wall controls the leak-off pressure, and because the leak-off pressure must overcome any tensile

strength of the formation (Addis et al., 1998). Nonetheless, it is widely accepted that the lower bound to leak-off pressures in vertical wells gives a reasonable estimate of the minimum horizontal stress (e.g. Bell, 1990; Breckels and van Eekelen, 1982).

A total of 40 closure pressures from minifrac tests conducted in 23 wells were combined with a large number of LOTs (Fig. 6). All of the LOTs conducted in the Cooper–Eromanga Basins are shallower than

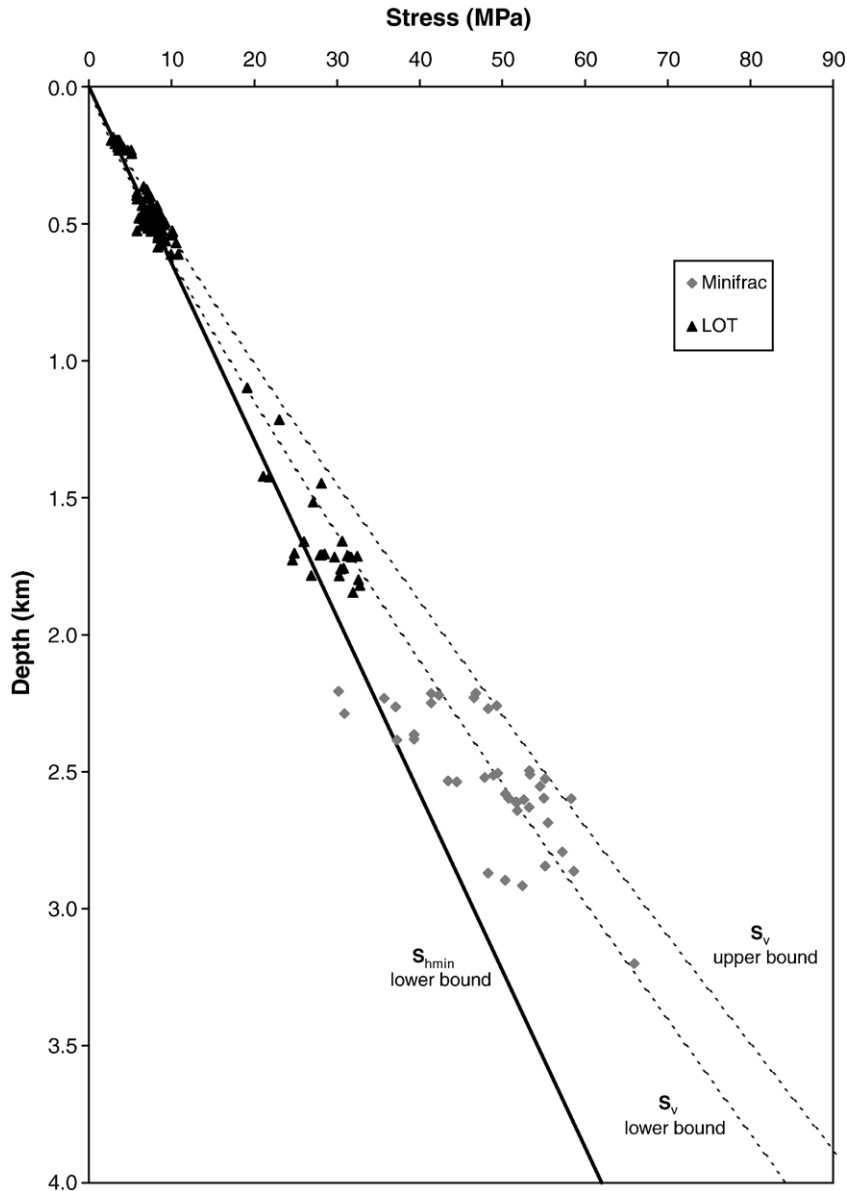


Fig. 6. Minimum horizontal stress (S_{hmin}) versus depth profile from a compilation of minifrac and LOT measurements for the Cooper–Eromanga Basins. A large degree of scatter is present in the minifrac measurements, which are considered to more reliably reflect S_{hmin} than the LOT data. Approximately half of the minifrac measurements coincide with the estimated bounds for S_v . We consider the scatter in the minifrac stress measurements that reflect genuine variation in S_{hmin} within the Cooper Basin.

2000 m in depth, while all of the minifrac data are greater than 2000 m in depth (Fig. 6). A depth versus stress plot displays significant scatter in the minifrac closure pressures across the basin (Fig. 6). Thus, it is not possible to display a single meaningful trend across the region. A lower bound estimate of the minimum horizontal stress (15.5 MPa/km) was determined using both the minifrac and the LOT data. All but two of the minifrac closure pressures are above the lower bound estimate for the minimum horizontal stress. The two closure pressures below the lower bound provide a poor estimate of the regional minimum horizontal stress, since they are not consistent with either the deeper minifrac data or the shallower LOT data. These two measurements may reflect the influence of local structure or interpretation from an ambiguous pressure versus time record.

A number of the closure pressures from the minifrac tests are as high as the vertical stress estimates (Fig. 6). Hence, the minimum horizontal stress may be greater than the vertical stress in some areas of the basins. As a consequence we have also determined the magnitude of the maximum horizontal stress assuming the vertical stress is the minimum principal stress (i.e. a reverse stress regime).

6. Maximum horizontal stress magnitude

The magnitude of the maximum horizontal stress (S_{Hmax}) is generally the most difficult component of the stress tensor to determine. In this study we have attempted to constrain the magnitude of the maximum horizontal stress using the frictional limit to stress and the presence of drilling-induced tensile fractures (DITFs) in certain wells. It is difficult to calculate a basin-wide estimate of the maximum horizontal stress using frictional limits because both the minimum horizontal stress and the vertical stress, upon which estimates of the maximum horizontal stress depend, vary significantly across the basins. As a result the maximum horizontal stress is poorly constrained at the basin-wide scale. However, we have also calculated the complete stress tensor in two wells, Dullingari North-8 and Bulyeroo-1, in order to demonstrate that the maximum horizontal stress can be tightly constrained on a case-by-case basis.

The frictional limit to stress, beyond which faulting occurs, provides an upper bound estimate for the maximum horizontal stress. The magnitude of the maximum horizontal stress can be constrained in strike-slip and reverse faulting stress regimes by assuming that the ratio of the maximum to minimum

effective principal stress cannot exceed that required to cause faulting on an optimally oriented, pre-existing, cohesionless fault (Sibson, 1974). The frictional limit to stress is given by:

$$\frac{S_1 - P_p}{S_3 - P_p} \leq \left\{ \sqrt{(\mu^2 + 1)} + \mu \right\}^2, \quad (4)$$

where μ is the coefficient of friction on an optimally oriented, cohesionless pre-existing fault, S_1 is the maximum principal stress, S_3 is the minimum principal stress and P_p is the pore pressure. For a typical value of $\mu = 0.6$ (Zoback and Healy, 1984):

$$\frac{S_1 - P_p}{S_3 - P_p} \leq 3.12. \quad (5)$$

This relationship can be used to estimate the magnitude of the maximum principal stress in seismically active regions (Zoback and Healy, 1984) and provides an upper limit to the maximum principal stress in seismically inactive regions.

In both strike-slip and reverse fault stress regimes the maximum horizontal stress is the maximum principal stress and hence can be calculated using the frictional limit to stress (Eq. (5)). However, in a normal fault stress regime the maximum horizontal stress is the intermediate principal stress (S_2) and cannot be estimated using Eq. (5). Taking the lower bound value for the minimum horizontal stress (15.5 MPa/km), the frictional limit calculation yields an S_1 gradient of 27 MPa/km (108 MPa at 4 km), which is in excess of the upper limit to the vertical stress (Fig. 7). Hence, if stresses are at the frictional limit, then even the areas of lower horizontal stress are subjected to a strike-slip (as opposed to normal) fault stress regime. Given that minifrac closure pressures are as high as the vertical stress, the highest possible value for S_3 in the region is the upper bound to the vertical stress (Eq. (3)). The corresponding estimate of the frictional limit of the maximum horizontal stress is not linear with depth (because the vertical stress is not linear with depth), but is approximately 91 MPa at 2 km and 205 MPa at 4 km depth. Thus, the frictional limit to the maximum horizontal stress varies between 108 MPa and 205 MPa at 4 km depth in the Cooper–Eromanga Basins.

The presence of drilling-induced tensile fractures (DITFs) in a vertical well provides additional constraint on the magnitude of the maximum horizontal stress. Drilling-induced tensile fractures form in the orientation of the maximum horizontal stress when the circumferential stress around the wellbore is less than the tensile strength of the rock (Brudy and Zoback, 1999). They are

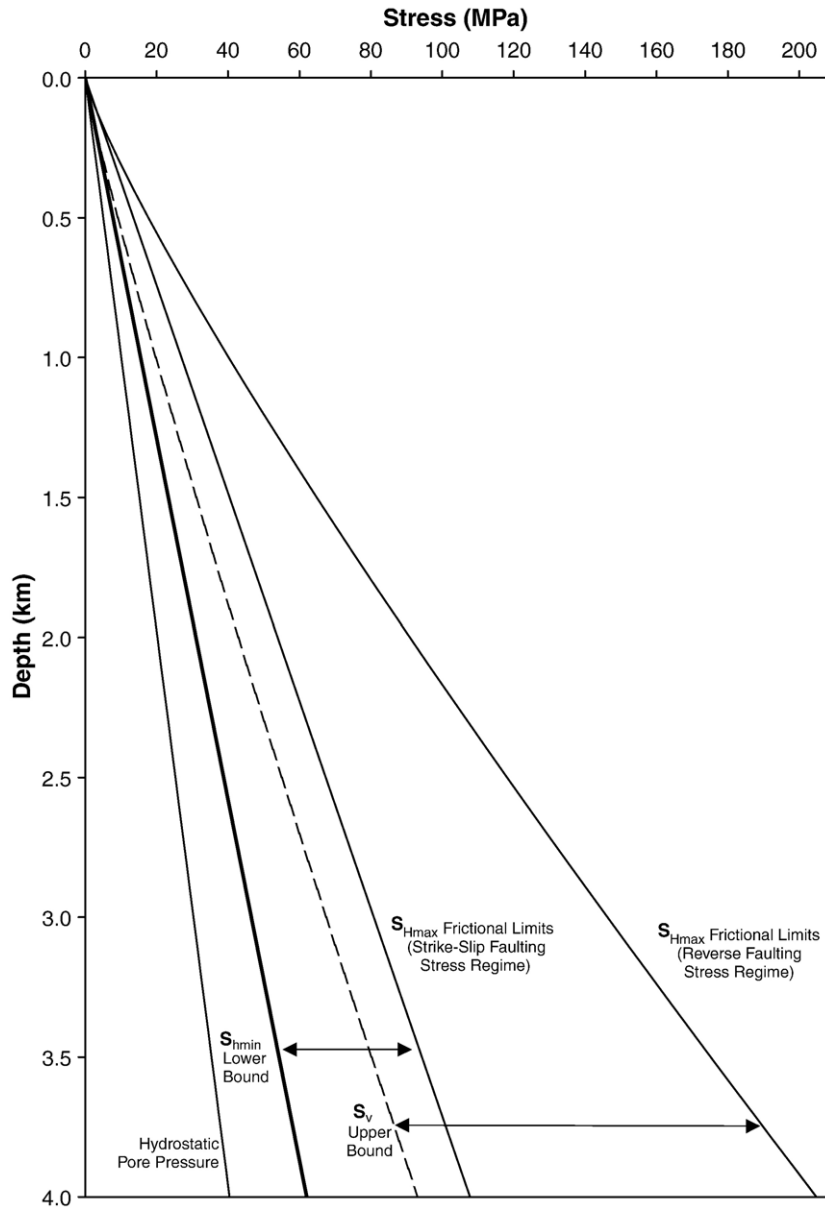


Fig. 7. Stress versus depth plot showing lower bound for S_{Hmax} (assuming S_{hmin} lower bound is minimum principal stress i.e. strike-slip fault stress regime) and upper bound for S_{Hmax} (assuming S_v upper bound is the minimum principal stress i.e. a reverse fault stress regime). Lines with arrowheads indicate the minimum principal stress from which the maximum horizontal stress was calculated.

dark in colour (high conductivity) as they are filled by drilling mud and generally have well defined edges. Drilling-induced tensile fractures have been interpreted in 27 wells, spread over most of the Cooper Basin (Reynolds et al., 2005). The presence of DITFs in near vertical wells, such as in the Cooper Basin, requires a large difference between the magnitude of the minimum and maximum horizontal stresses and they mainly form in a strike-slip fault stress regime (Moos and Zoback,

1990; Peska and Zoback, 1995). The circumferential stress around a vertical wellbore ($\sigma_{\theta\theta}$) is represented by:

$$\sigma_{\theta\theta} = S_{Hmax} + S_{hmin} - 2(S_{Hmax} - S_{hmin})\cos 2\theta - P_p - P_w \quad (6)$$

where θ is the angle around the wellbore wall measured from the direction of the maximum horizontal stress, P_p is the pore pressure and P_w is the mud weight. Thermal

stresses around the wellbore, due to the cooler drilling mud, were not included in the calculation of the circumferential stress (Eq. (6)), since the required data was not available. The thermal stress induce extensional stresses at the wellbore wall (Moos and Zoback, 1990), thus promoting the formation of DITFs. In order to counteract the thermal effect we have assumed that the rocks have zero tensile strength. This allows for a few MPa of thermal effect given the tensile strength of rocks in the basin that ranges between 4 MPa and 16 MPa (Nelson et al., submitted for publication).

A DITF forms at the orientation of the maximum horizontal stress and hence $\theta=0^\circ$ in Eq. (6). As mentioned above we have assumed that the rocks in the area have zero tensile strength (i.e. $\sigma_{\theta\theta}=0$ when $\theta=0^\circ$). Thus, Eq. (6) can be reduced to:

$$S_{Hmax} \geq 3S_{Hmin} - P_p - P_w. \quad (7)$$

In areas where DITFs occur we are able to constrain a lower bound estimate for the maximum horizontal stress. We have not used DITFs to constrain the magnitude of the maximum horizontal stress in a regional sense, since DITFs have not been observed in all wells in the basin. Instead we have applied this technique to the two example wells below.

7. Stress tensor at Dullingari North-8 and Bulyeroo-1

The previous three sections have demonstrated that the vertical stress and minimum horizontal stress vary across the basins. Hence, the maximum horizontal stress cannot be well constrained for the basins as a whole using frictional limits. However, the maximum horizontal stress can be more tightly constrained at specific locations by determining the stress tensor from data in a single well or data in a number of nearby wells. In this study we have determined the full stress tensor for Bulyeroo-1, located in the Nappamerri Trough, and Dullingari North-8, located on the southern side of the Nappacoongee Ridge (Fig. 1). These two wells were selected because both wells provide a data set from which the full stress tensor can be determined and furthermore they are located in different structural settings within the Cooper Basin (i.e. trough versus ridge). Both wells have image log data from Schlumberger's Formation MicroScanner (FMS) tool. A large number of borehole breakouts and DITFs were interpreted from the image logs in these wells (Reynolds et al., 2005) (Figs. 8 and 9). The weighted average maximum horizontal stress orienta-

tion for Bulyeroo-1 is 087°N and for Dullingari North-8 is 095°N (Reynolds et al., 2005).

Direct pore pressure measurements were not conducted in either Dullingari North-8 or Bulyeroo-1. Tests from other wells close to Dullingari North-8 provide no evidence of overpressure in this part of the Cooper Basin. Thus, we have assumed hydrostatic pore pressure for the analysis of Dullingari North-8 (Fig. 8). Mud weights used in Bulyeroo-1 suggest that overpressure occurs below approximately 3 km in depth (Fig. 9). A number of other wells in the Nappamerri Trough also show signs of overpressure (van Ruth and Hillis, 2000). Hence, we have assumed the pore pressure is equal to the mud weight in Bulyeroo-1 in order to calculate the maximum horizontal stress magnitude. Static mud weights were used to calculate the maximum horizontal stress from the DITFs, since no information on equivalent circulating densities (ECD) exists for the two wells. Equivalent circulating densities are larger than static mud weights due to the circulation of the drilling mud during drilling. Thus, static mud weights may over-estimate the magnitude of the maximum horizontal stress. Nonetheless, we consider it appropriate to use static mud weights for the two wells in this study due to the extensive number of DITFs throughout the image log section of the wells.

Three minifrac tests were conducted in Dullingari North-8 at depths over which the image log was run (Fig. 8). The two deeper minifrac tests were conducted in the Patchawarra Formation and the shallower test in the Toolachee Formation (Fig. 8). The minimum horizontal stress estimates from the two deeper minifrac tests were used to approximate a linear minimum horizontal stress trend (20 MPa/km). The shallower minifrac conducted does not sit on the same trend as defined by the two deeper minifrac tests. Thus, the minimum horizontal stress gradient is higher in the Patchawarra Formation than in the Toolachee Formation and hence, stress measurements in the Patchawarra Formation cannot be extrapolated to the Toolachee Formation. Four minifrac tests were conducted in Bulyeroo-1 at depths over which the image log was run (Fig. 9). Two minifrac tests were conducted in the Daralingie Formation and one each in the Toolachee Formation and the Nappamerri Group. The minimum horizontal stress magnitude is approximated by a linear trend (20.5 MPa/km) defined from three of the four minifrac tests. One of the minifrac tests in the Daralingie Formation has a lower closure pressure gradient and was excluded from the calculation of the minimum horizontal stress trend because it was conducted in an interval including coals, which exhibit anomalously low

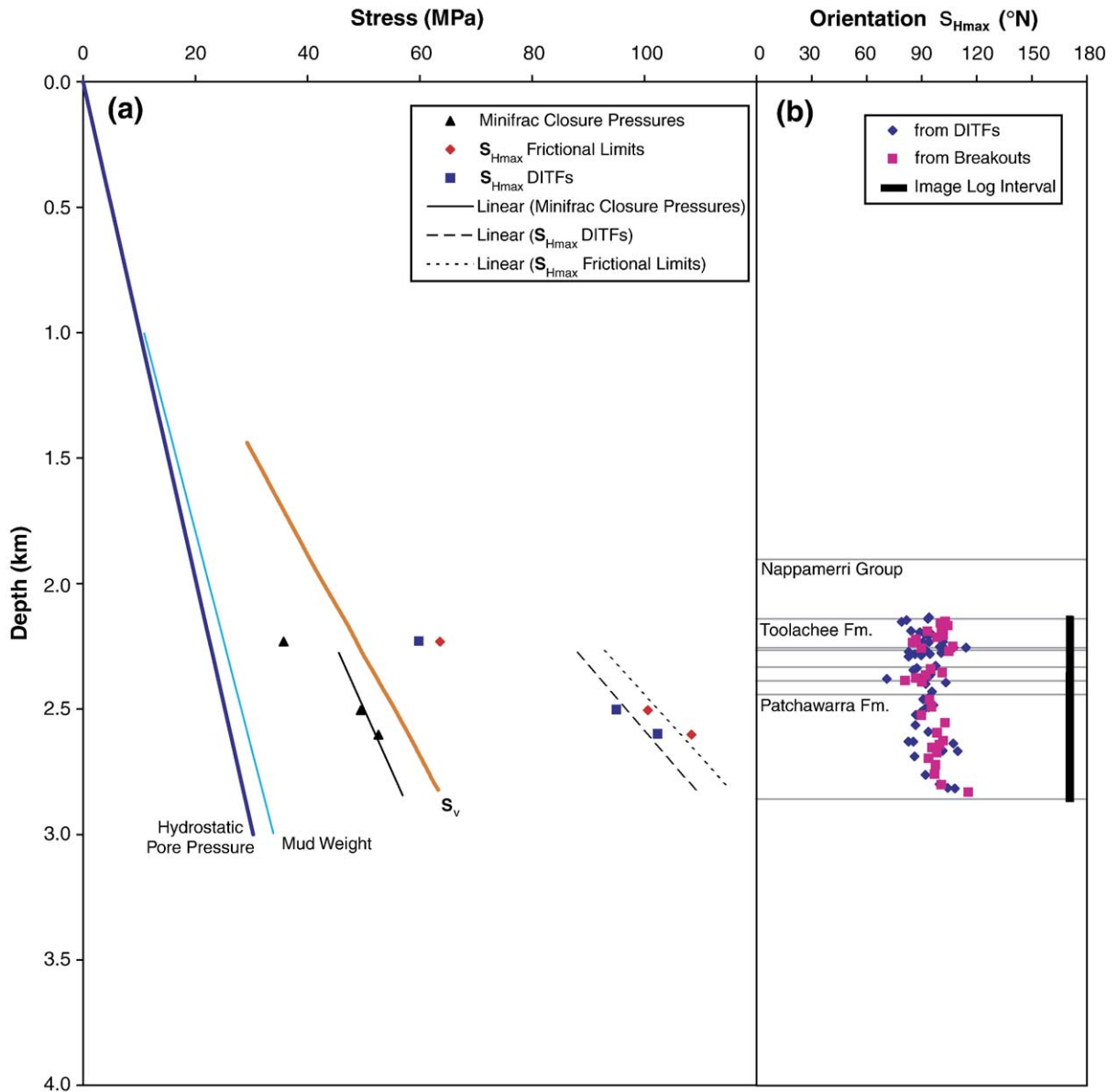


Fig. 8. (a) Stress versus depth and (b) orientation of S_{Hmax} versus depth plots for Dullingari North-8. Stratigraphy between Toolachee and Patchawarra Formations include, from top to bottom, Daralingie Formation, Roseneath Shale, Epsilon Formation and Murteree Shale. The vertical stress (S_v) calculated from density log run in nearby well Dullingari North-4.

stresses. The minimum horizontal stress estimates from Bulyeroo-1 and Dullingari North-8 both demonstrate that lithology is a key influence on the minimum horizontal stress magnitude in the Cooper Basin and that the mechanical stratigraphy of the basin affects stress magnitudes (cf. Teufel, 1991).

No density log was run in Dullingari North-8 and thus a vertical stress profile could not be calculated for the well. Nevertheless, for this study we have used the vertical stress calculated in a nearby well,

Dullingari North-4, to approximate the vertical stress profile in Dullingari North-8 (Fig. 8). A density log was run in Bulyeroo-1 and a corresponding vertical stress profile was calculated (Fig. 9). The vertical stress magnitude for both wells are slightly higher than the minimum horizontal stress as estimated from the minifrac tests.

The upper bound estimate of the maximum horizontal stress was calculated using the frictional limit to stress, with μ equal to 0.6, and was estimated to be

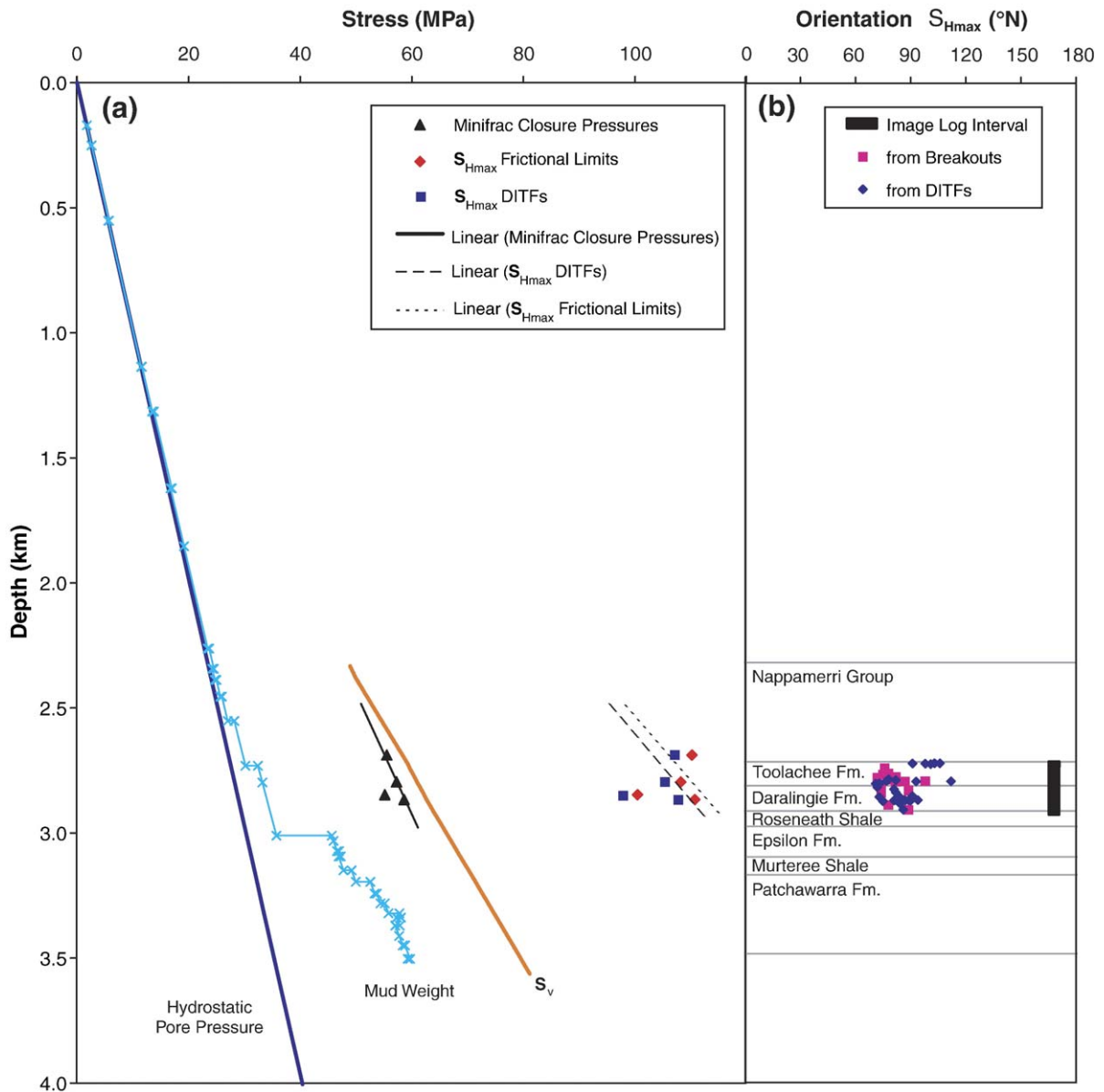


Fig. 9. (a) Stress versus depth and (b) orientation of S_{Hmax} versus depth plots for Bulyeroo-1.

41.1 MPa/km in Dullingari North-8 and 38.6 MPa/km in Bulyeroo-1. The lower bound estimate of the maximum horizontal stress magnitude was calculated using the presence of DITFs (Eq. (7)) and was estimated to be 38.8 MPa/km in Dullingari North-8 and 37.9 MPa/km in Bulyeroo-1. Stress magnitudes for the two wells have been calculated at a depth of 2.8 km and are listed in Table 1. In Dullingari North-8 the maximum horizontal stress has been constrained to between 108 MPa and 115 MPa at 2.8 km depth. In Bulyeroo-1 the maximum horizontal stress has been

constrained to between 106 MPa and 108 MPa at 2.8 km depth. The estimate of the maximum horizontal stress is more tightly constrained in Bulyeroo-1 than in Dullingari North-8. This is a result of the increased pore pressure in Bulyeroo-1 and the need to maintain the same ratio of the effective maximum horizontal stress ($S_{Hmax} - P_p$) to effective minimum horizontal stress ($S_{Hmin} - P_p$) in Eq. (5). As a consequence, the estimate of the maximum horizontal stress using frictional limits is reduced for increasing pore pressures. A strike-slip stress regime exists at the depth interval of

Table 1
Stress magnitudes determined at 2.8 km depth in Dulligari North-8 and Bulyeroo-1

Stress component	Dulligari North-8 (MPa)	Dulligari North-8 (MPa/km)	Bulyeroo-1 (overpressure) (MPa)	Bulyeroo-1 (overpressure) (MPa/km)
Mud weight	31	11.2	33	11.8
Pore pressure	28	10	33	11.8
Minimum horizontal stress	56	20	57	20.4
Vertical stress	63	22.5	61	21.8
Maximum horizontal stress (DITF)	108	38.6	106	37.9
Maximum horizontal stress (frictional limit)	115	41.1	108	38.6

Pore pressure in Bulyeroo-1 is assumed to be equal to the mud weight.

the image logs in both Dulligari North-8 and Bulyeroo-1 (Figs. 10 and 11).

8. Discussion

This study demonstrates that the magnitude of the maximum horizontal stress cannot be tightly constrained across the Cooper–Eromanga Basins as a whole. However, the maximum horizontal stress can be tightly constrained in individual wells, as demonstrated at

Dulligari North-8 and Bulyeroo-1. The maximum horizontal stress is the maximum principal stress in the Cooper–Eromanga Basins, and is significantly greater in magnitude than both the minimum horizontal stress and the vertical stress. Results from minifrac tests and LOTs indicate that the magnitude of the minimum horizontal stress is generally less than the vertical stress magnitude. A strike-slip fault ($S_{Hmax} > S_v > S_{hmin}$) stress regime dominates in the Cooper–Eromanga Basins at a depth of 1 to 3 km. The minifrac data also indicate that

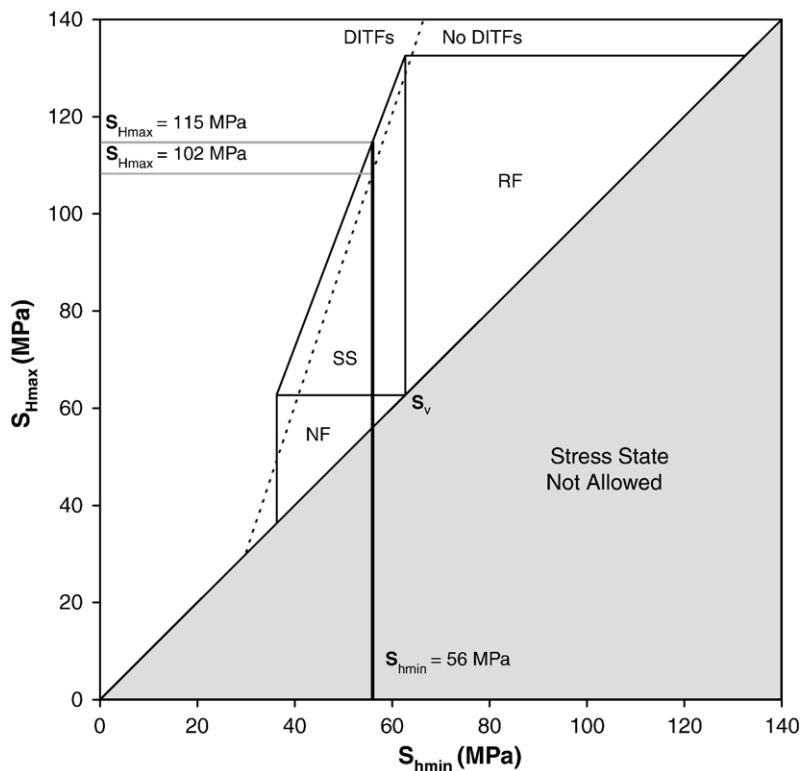


Fig. 10. Allowable stress region diagram for Dulligari North-8 at a depth of 2.8 km with hydrostatic pore pressure (after Moos and Zoback, 1990). The upper and lower limits for S_{Hmax} are constrained by frictional limit to stress and the presence of DITFs. NF: normal fault stress regime, SS: strike-slip fault stress regime, RF: reverse fault stress regime.

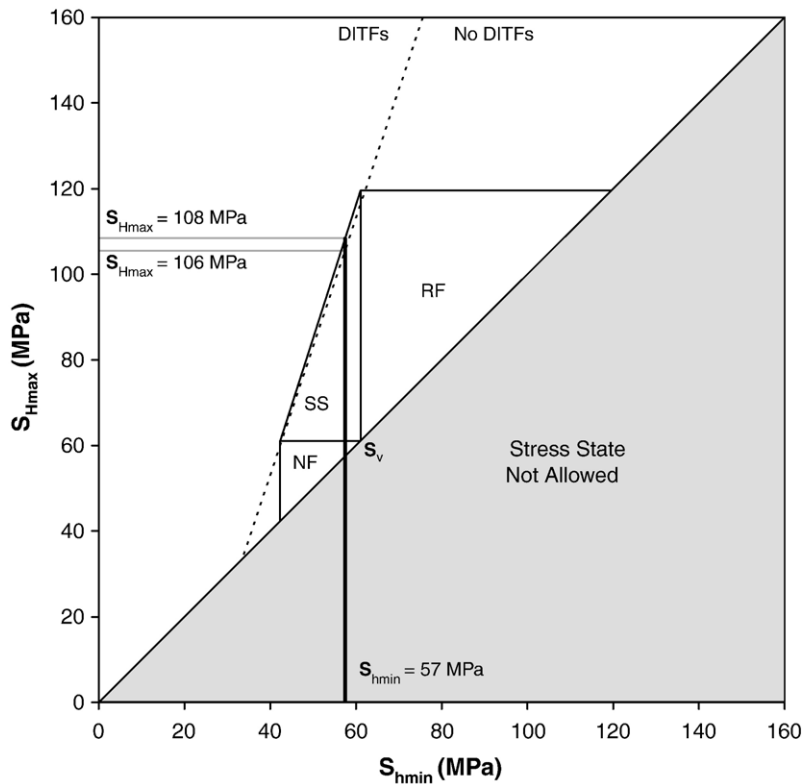


Fig. 11. Allowable stress region diagram for Bulyeroo-1 at a depth of 2.8 km with the pore pressure equal to the mud weight (after Moos and Zoback, 1990). The upper and lower limits for S_{Hmax} are constrained by frictional limit to stress and the presence of DITFs. NF: normal fault stress regime, SS: strike-slip fault stress regime, RF: reverse fault stress regime.

in some areas the minimum horizontal stress may be as high as the vertical stress such that the stress regime is on the border of strike-slip faulting and reverse faulting ($S_{Hmax} > S_v \approx S_{hmin}$). This result is consistent with most other intraplate regions, which are characterized by either strike-slip or reverse faulting stress regimes (Zoback, 1992).

The differential stress ($S_1 - S_3$) in a strike-slip stress regime is the difference between the maximum and minimum horizontal stresses ($S_{Hmax} - S_{hmin}$). Stress magnitudes determined at Dullingari North-8 indicate that the differential stress in the Cooper Basin is particularly high, being ~ 50 MPa at 2.8 km depth. The high differential stress is also manifested by the co-occurrence of borehole breakouts and DITFs in many vertical wells and by the strongly developed east–west maximum horizontal stress orientation throughout the Cooper Basin (Reynolds et al., 2005).

High differential stress has also been observed elsewhere in Australia, including within the West Tuna field in the Gippsland Basin (Nelson and Hillis, 2005). The Gippsland Basin is located offshore Victoria, approximately 1400 km southeast of the Cooper–

Eromanga Basins. In an equivalent study of the West Tuna field, Nelson and Hillis (2005) show that the vertical stress is 22 MPa/km (at 3000 m), the minimum horizontal stress is 20 MPa/km and the maximum horizontal stress is between 39 and 42 MPa/km. These gradients imply a differential stress of approximately 54 MPa at 2.8 km depth. Plate-scale stress modelling suggests that the in situ stress field in the Gippsland Basin, and much of southeastern Australia, is strongly influenced by the increased coupling of the Australian and Pacific plate boundary at New Zealand since the late Miocene (Sandiford et al., 2004). Hence, the high differential stress in the Gippsland Basin is probably a result of the proximity of the basin to the oblique compression occurring along the New Zealand plate boundary (Nelson and Hillis, 2005).

Despite an increase in the uncertainty of the maximum horizontal stress with depth, it is clear that the differential stress in the Cooper–Eromanga Basins, an area of high surface heat flow, is substantial. A number of locations worldwide, including the KTB drill site in Germany (Brudy et al., 1997), show evidence of large differential stresses in the upper crust. The results

from the KTB site indicate that in areas of moderately high heat flow the upper brittle part of the crust is strong and able to support forces equivalent in magnitude to those driving the plates (Zoback et al., 1993). This is because the relatively high temperature in the lower crust and upper mantle can only support a limited amount of force before creep occurs (Kusznir and Park, 1984). Thus, the cumulative lithospheric strength is largely due to the brittle upper crust (Kusznir, 1991). This process has been referred to as stress amplification (Bott and Kusznir, 1984) and the upper crustal stress guide (Zoback et al., 2002).

A high-strength upper crust provides a means to transfer tectonic stress over thousands of kilometres in intraplate regions (Kusznir and Bott, 1977; Zoback et al., 2002). The transfer of tectonic stresses over large intraplate regions has been identified in a number of continents (e.g. North and South America and Western Europe) from consistent maximum horizontal stress orientations that are aligned with the direction of absolute plate velocity (Richardson, 1992; Zoback and Zoback, 1991; Zoback et al., 1989). However, the regional east–west maximum horizontal stress orientation in the Cooper–Eromanga Basins is orthogonal to the absolute direction of plate velocity for the Indo-Australian plate indicating that plate-driving forces, such as ridge-push, do not control the in situ stress field in the Cooper–Eromanga Basins (Reynolds et al., 2005).

We propose that the in situ stress field in the Cooper–Eromanga Basins is a direct result of the complex interaction of tectonic stresses from the convergent plate boundaries surrounding the Indo-Australian plate that are transmitted into the center of the plate through the high-strength upper crust. An obvious source of the tectonic stress is from the convergent plate boundary at New Zealand. The high crustal strength in the Gippsland Basin provides a means for the tectonic stresses at the New Zealand plate boundary to propagate into the interior of the Indo-Australian plate. However, finite element modelling of tectonic forces acting on the Indo-Australian plate indicates that forces from a number of plate boundaries contribute to the east–west maximum horizontal stress orientation in the Cooper–Eromanga Basins (Reynolds et al., 2002). Thus, the high differential stress in the Cooper–Eromanga Basins is likely the result of tectonic forces from a number of plate boundaries in addition to the New Zealand plate boundary zone.

Previous tectonic force modelling by Reynolds et al. (2002) has matched the regional east–west maximum horizontal stress orientation in the Cooper–Eromanga Basins, but does not match the stress magnitude results present here. The modelling produces a relatively

isotropic horizontal stress field ($S_{Hmax} \approx S_{Hmin}$) in central Australia in order to match the east–west stress orientation in the Cooper–Eromanga Basins. Improvement of the plate-scale modelling is required to match both the east–west maximum horizontal stress orientation and the highly anisotropic horizontal stress field ($S_{Hmax} \gg S_{Hmin}$).

The high differential stress determined for the Cooper–Eromanga Basins is consistent with theoretical calculations of differential stress for a strike-slip stress regime with hydrostatic pore pressure and a moderately high heat flow (Brudy et al., 1997; Zoback et al., 1993). In addition, the high-strength upper crustal model outlined by Zoback et al. (1993) for the KTB site in Germany predicts higher seismicity rates in the overlying brittle crust. However, only a minor amount of seismic activity has been recorded in the Cooper–Eromanga Basins when compared to other areas of Australia. Thus, the strain rate for the region appears to be fairly low. One possible explanation of the lack of seismicity in the Cooper–Eromanga Basins is that the deformation is focussed in the Flinders Ranges, which lies directly south of the Cooper–Eromanga Basins. The Flinders Ranges is one of Australia's most seismically active regions. Seismicity occurs in a band parallel to the north–south structure of the ranges and also coincides with part of an area of high heat flow, known as the South Australian Heat Flow Anomaly (Neumann et al., 2000). A high strain rate of up to 10^{-16} s^{-1} has been estimated for the Flinders Ranges from seismic moment release rates (Sandiford et al., 2004). Currently no stress magnitude data exists for the Flinders Ranges, so we are unable to determine whether the crust in the region is in fact stronger or weaker than the crust in the Cooper–Eromanga Basins. Obtaining stress magnitude data in the Flinders Ranges would significantly help our understanding of intraplate deformation in Australia and should be seen as a priority in order to improve seismic hazard assessment.

9. Summary

In this study we have constrained the magnitude of the vertical stress, the minimum horizontal stress and the maximum horizontal stress for the Cooper–Eromanga Basins. The vertical stress and the minimum horizontal stress exhibit a reasonable degree of variability across the basins. In general, a strike-slip fault stress regime ($S_{Hmax} > S_v > S_{Hmin}$) dominates the Cooper–Eromanga Basins. However, in some areas of the basins the magnitude of the minimum horizontal stress is as high or potentially greater than the vertical stress. The

magnitude of the maximum horizontal stress was constrained by the frictional limits to stress beyond which faulting occurs and by the presence of DITFs in some areas. Significant variation in the magnitude of the maximum horizontal stress is estimated to occur across the basins as a whole. Thus, it is inappropriate to use a single stress tensor for geomechanical modelling of the whole basin. Nonetheless the stress tensor can be tightly constrained on a well-by-well basis, as demonstrated by stress estimates at Bulgeroo-1 and Dullingari North-8. The stress tensors for these two wells indicate a high differential stress, which is also reflected across the basin as a whole by the presence of DITFs in 27 wells and the consistent maximum horizontal stress orientation (Reynolds et al., 2005). The large differential stress in the Cooper–Eromanga Basins implies a high strength upper crust for the region. We propose that the large differential stress is a result of tectonic stresses that have propagated through the Indo-Australian plate from a number of convergent plate boundaries, such as New Zealand. Stress magnitude estimates in the Cooper–Eromanga Basins have significant implications for our understanding of the controls on the present-day stress field of Australia and the source of intraplate seismicity. Consequently, further improvement of the stress models of Australia should focus on matching the observed stress field in central Australia and in particular the Cooper–Eromanga Basins.

Acknowledgements

The authors wish to thank Santos and their joint venture partners, Delhi Petroleum, Origin Energy, Gulf (Australia) and Basin Oil for providing data and allowing publication of the results. Primary Industries and Resources South Australia is also thanked for providing access to image log data. Mike Sandiford, John Reinecker and an anomalous reviewer are thanked for their comments that helped to refocus this manuscript. The depth to basement map for the Cooper Basin was kindly provided by Primary Industries and Resources South Australia, Queensland Department of Mines and Energy, Northern Territory Department of Mines and Energy, Mineral Resources New South Wales and Geoscience Australia. This research has been part of the Australasian Stress Map project funded by an Australian Research Council grant.

References

- Addis, M.A., Hanssen, T.H., Yassir, N., Willoughby, D.R., Enever, J., 1998. A comparison of leak-off test and extended leak-off test data

- for stress estimation. *Eurock 98 Rock Mechanics in Petroleum Engineering*, Trondheim, Norway, pp. 131–140.
- Apak, S.N., Stuart, W.J., Lemon, N.M., Wood, G., 1997. Structural evaluation of the Permian–Triassic Cooper Basin, Australia: relation to hydrocarbon trap styles. *AAPG Bull.* 81, 533–555.
- Bell, J.S., 1990. The stress regime of the Scotian Shelf offshore eastern Canada to 6 kilometres depth and implications for rock mechanics and hydrocarbon migration. In: Maury, V., Fourmaintraux, D. (Eds.), *Rock at Great Depth*. Balkema, Rotterdam, pp. 1243–1265.
- Bott, M.H.P., Kusznir, N.J., 1984. The origin of tectonic stress in the lithosphere. *Tectonophysics* 105, 1–13.
- Breckels, I.M., van Eekelen, H.A.M., 1982. Relationship between horizontal stress and depth in sedimentary basins. *J. Pet. Technol.* 34, 2191–2198.
- Brudy, M., Zoback, M.D., 1999. Drilling-induced tensile wall-fractures: implications for determination of in-situ stress orientation and magnitude. *Int. J. Rock Mech. Min. Sci.* 36, 191–215.
- Brudy, M., Zoback, M.D., Fuchs, K., Rummel, F., Baumgartner, J., 1997. Estimation of the complete stress tensor to 8 km depth in the KTB scientific drill holes: implications for crustal strength. *J. Geophys. Res.* 102, 18453–18475.
- Chipperfield, S.T., Britt, L.K., 2000. Application of after-closure analysis for improved fracture treatment optimisation: a Cooper Basin case study. *SPE Rocky Mountain Regional/Low Permeability Reservoirs Symposium*, Denver, Colorado, pp. 1–15.
- Enever, J.R., 1993. Case studies of hydraulic fracture stress measurement in Australia. In: Hudson, J.A. (Ed.), *Comprehensive Rock Engineering, Rock Testing and Site Characterization*. *Comprehensive Rock Engineering: Principles, Practice, and Projects*. Pergamon Press, New York, pp. 497–532.
- Gravestock, D.I., Jensen-Schmidt, B., 1998. Structural setting. In: Gravestock, D.I., Hibbert, J.E., Drexel, J.F. (Eds.), *Petroleum Geology of South Australia, Volume 4: Cooper Basin*. Department of Primary Industries and Resources, pp. 47–67.
- Gronseth, J.M., Kry, P.R., 1983. Instantaneous shut-in pressure and its relationship to the minimum in-situ stress. *Proc. Hydraulic Fracturing Stress Measurements*, Monterey. National Academy Press, Washington, DC, pp. 55–60.
- Hill, A.J., Gravestock, D.I., 1995. Cooper Basin. In: Drexel, J.F., Preiss, W.V. (Eds.), *The Geology of South Australia, Vol. 2, The Phanerozoic*. South Australian Geological Survey Bulletin, pp. 78–87.
- Hillis, R.R., Reynolds, S.D., 2000. The Australian stress map. *J. Geol. Soc. (Lond.)* 157 (5), 915–921.
- Johnson, R.L., Aw, K.P., Ball, D., Willis, M., 2002. Completion, perforating and hydraulic fracturing design changes yield success in an area of problematic frac placement—the Cooper Basin, Australia. *SPE Asia Pacific Oil and Gas Conference and Exhibition*, Melbourne, Australia, pp. 1–18.
- Johnson, R.L., Greenstreet, C.W., 2003. Managing uncertainty related to hydraulic fracturing modeling in complex stress environments with pressure-dependent leak off. *SPE Annual Technical Conference and Exhibition*, Denver, Colorado, USA, pp. 1–15.
- Kusznir, N.J., 1991. The distribution of stress with depth in the lithosphere: thermo-rheological and geodynamic constraints. *Philos. Trans. R. Soc. Lond., Ser. A Phys. Sci. Eng.* 337, 95–110.
- Kusznir, N.J., Bott, M.H.P., 1977. Stress concentration in the upper lithosphere caused by underlying viscoelastic creep. *Tectonophysics* 43, 247–256.
- Kusznir, N.J., Park, R.G., 1984. The strength of intraplate lithosphere. *Phys. Earth Planet. Inter.* 36, 224–235.

- Laws, R.A., Gravestock, D.I., 1998. Introduction. In: Gravestock, D.I., Hibbert, J.E., Drexel, J.F. (Eds.), *Petroleum Geology of South Australia, Volume 4: Cooper Basin*. Department of Primary Industries and Resources, pp. 1–6.
- Ludwig, W.J., Nafe, J.E., Drake, C.L., 1970. Seismic refraction. In: Maxwell, A.E. (Ed.), *The Sea: Ideas and Observations on Progress in the Study of the Seas, Vol. 4: New Concepts of Sea Floor Evolution*. Wiley-Interscience, New York, pp. 53–84.
- Mithen, D.P., 1982. Stress amplification in the upper crust and the development of normal faulting. *Tectonophysics* 83, 259–273.
- Moos, D., Zoback, M.D., 1990. Utilization of observations of well bore failure to constrain the orientation and magnitude of crustal stresses: application to continental, deep sea drilling project and ocean drilling program boreholes. *J. Geophys. Res.* 95 (B6), 9305–9325.
- Nelson, E.J., Hillis, R.R., 2005. In situ stresses of the West Tuna area, Gippsland Basin. *Aust. J. Earth Sci.* 52 (2), 299–313.
- Nelson, E.J., Chipperfield, S.T., Hillis, R.R., Gilbert, J., McGowen, J., Mildren, S.D., submitted for publication. The relationship between closure pressures identified from fluid injections and the minimum principal stress in strong rocks. *Int. J. Rock Mech. Min. Sci.*
- Neumann, N., Sandiford, M., Foden, J., 2000. Regional geochemistry and continental heat flow; implications for the origin of the South Australian heat flow anomaly. *Earth Planet. Sci. Lett.* 183 (1–2), 107–120.
- Peska, P., Zoback, M.D., 1995. Compressive and tensile failure of inclined well bores and determination of in situ and rock strength. *J. Geophys. Res.* 100 (B7), 12791–12811.
- Reynolds, S.D., Coblenz, D.D., Hillis, R.R., 2002. Tectonic forces controlling the regional intraplate stress field in continental Australia: results from new finite-element modelling. *J. Geophys. Res.* 107 (B7). doi:10.1029/2001JB000408.
- Reynolds, S.D., Coblenz, D.D., Hillis, R.R., 2003. Influences of plate-boundary forces on the regional intraplate stress field of continental Australia. In: Hillis, R.R., Müller, R.D. (Eds.), *Evolution and Dynamics of the Australian Plate*, pp. 59–70.
- Reynolds, S.D., Mildren, S.D., Hillis, R.R., Meyer, J.J., Flottmann, T., 2005. Maximum horizontal stress orientations in the Cooper Basin, Australia: implications for plate scale tectonics and local stress sources. *Geophys. J. Int.* 150, 331–343.
- Richardson, R.M., 1992. Ridge forces, absolute plate motions, and the intraplate stress field. *J. Geophys. Res.* 97 (B8), 11739–11748.
- Roberts, G.A., Chipperfield, S.T., Miller, W.K., 2000. The evolution of a high-wellbore pressure loss treatment strategy for the Australian Cooper Basin. SPE Annual Technical Conference and Exhibition, Dallas, Texas, pp. 1–12.
- Sandiford, M., Wallace, M., Coblenz, D., 2004. Origin of the in situ stress field in south-eastern Australia. *Basin Res.* 16, 325–338.
- Sibson, R.H., 1974. Frictional constraints on thrust, wrench and normal faults. *Nature* 249, 542–544.
- Somerville, M., Wyborn, D., Chopra, P., Rahman, S., Estrella, D., Van der Meulen, T., 1994. *Hot Dry Rocks Feasibility Study*, Canberra, ACT.
- Teufel, L.W., 1991. Influence of lithology and geologic structure on in situ stress: examples of stress heterogeneity in reservoirs. In: Lake, L.W., Carroll, H.B., Wesson, T.C. (Eds.), *Reservoir Characterization II*, San Diego, CA, United States, pp. 565–578.
- van Ruth, P., Hillis, R., 2000. Estimating pore pressure in the Cooper Basin, South Australia: sonic log method in an uplifted basin. *Explor. Geophys.* 31, 441–447.
- Wyborn, D., de Graaf, L., Davidson, S., Hann, S., 2004. Development of Australia's first hot fractured rock (HFR) underground heat exchanger, Cooper Basin, South Australia. In: Boulton, P.J., Johns, D.R., Lang, S.C. (Eds.), *Eastern Australasian Basins Symposium II*. Petroleum Exploration Society of Australia, Adelaide, pp. 423–430.
- Zoback, M.L., 1992. First- and second-order patterns of stress in the lithosphere: the world stress map project. *J. Geophys. Res.* 97 (B8), 11703–11728.
- Zoback, M.D., Healy, J.H., 1984. Friction, faulting and in situ stress. *Ann. Geophys.* 2 (6), 689–698.
- Zoback, M.D., Zoback, M.L., 1991. Tectonic stress field of North America and relative plate motion. In: Slemmons, D.B., Engdahl, E.R., Zoback, M.D., Blackwell, D.D. (Eds.), *Neotectonics of North America*. Geological Society of America, Boulder, CO, pp. 339–366.
- Zoback, M.L., Zoback, M.D., Adams, J., Assumpcao, M., Bell, S., Bergman, E.A., Blumling, P., Bereton, N.R., Denham, D., Ding, J., Fuchs, K., Gay, N., Gregersen, S., Gupta, H.K., Gvishiani, A., Jacob, K., Klein, R., Knoll, P., Magee, M., Mercier, J.L., Muller, B. C., Paquin, C., Rajendran, K., Stephansson, O., Suarez, G., Suter, M., Udias, A., Xu, Z.H., Zhizhin, M., 1989. Global patterns of tectonic stress. *Nature* 341, 291–298.
- Zoback, M.D., Apel, R., Baumgartner, J., Brudy, M., Emmermann, R., Engeser, B., Fuchs, K., Kessels, W., Rischmuller, H., Rummel, F., Vernik, L., 1993. Upper-crustal strength inferred from stress measurements to 6 km depth in the KTB borehole. *Nature* 365, 633–636.
- Zoback, M.D., Townend, J., Grollimund, B., 2002. Steady-state failure equilibrium and deformation of intraplate lithosphere. *Int. Geol. Rev.* 44, 382–401.